

MICROCOPY RESOLUTION TEST CHART
NATIONAL BUREAU OF STANDARDS 1963-A

12

AD-A149 082

Final Report
Technical Report No. 10
Contract No.: US NAVY-N-00014-80-K-0969

Effect of Powder Characteristics
on Microstructure and Properties
in Alkoxide Prepared PZT Ceramics



DTIC
ELECTE
JAN 10 1985
B

DTIC FILE COPY

DEPARTMENT OF CERAMIC ENGINEERING
UNIVERSITY OF ILLINOIS
URBANA, ILLINOIS

DISTRIBUTION STATEMENT A
Approved for public release
Distribution Unlimited

84 12 14 02 8

REPRODUCED AT GOVERNMENT EXPENSE

Final Report
Technical Report No. 10
Contract No.: US NAVY-N-00014-80-K-0969

Effect of Powder Characteristics
on Microstructure and Properties
in Alkoxide Prepared PZT Ceramics

by

R. C. Buchanan and J. Boy

December 1984

Department of Ceramic Engineering
University of Illinois at Urbana-Champaign
105 S. Goodwin Avenue
Urbana, IL 61801

DTIC
ELECTE
JAN 10 1985
S D
B

Research was supported by the Office of Naval Research
Department of the Navy
Contract No. US NAVY-N-00014-80-K-0969

Production in whole or in part is permitted for any purpose
of the United States Government

DISTRIBUTION STATEMENT A
Approved for public release
Distribution Unlimited

REPORT DOCUMENTATION PAGE

1a. REPORT SECURITY CLASSIFICATION Unclassified		1b. RESTRICTIVE MARKINGS	
2a. SECURITY CLASSIFICATION AUTHORITY		3. DISTRIBUTION/AVAILABILITY OF REPORT Wid doc and at	
2b. DECLASSIFICATION/DOWNGRADING SCHEDULE		<div style="border: 1px solid black; padding: 5px; display: inline-block;"> DISTRIBUTION STATEMENT A Approved for public release Distribution Unlimited </div> to defense and organiza furnished	
4. PERFORMING ORGANIZATION REPORT NUMBER(S) Report #10		5. MOI Office of Naval Research US NAVY-N-00014-80-K-0969	
6a. NAME OF PERFORMING ORGANIZATION University of Illinois	6b. OFFICE SYMBOL (If applicable)	7a. NAME OF MONITORING ORGANIZATION ONR	
6c. ADDRESS (City, State and ZIP Code) Department of Ceramic Engineering 105 S. Goodwin Avenue Urbana, IL 61801		7b. ADDRESS (City, State and ZIP Code)	
8a. NAME OF FUNDING/SPONSORING ORGANIZATION Office of Naval Research	8b. OFFICE SYMBOL (If applicable)	9. PROCUREMENT INSTRUMENT IDENTIFICATION NUMBER	
8c. ADDRESS (City, State and ZIP Code) Division of Materials Research Arlington, VA 22217		10. SOURCE OF FUNDING NOS.	
		PROGRAM ELEMENT NO.	PROJECT NO.
		TASK NO.	WORK UNIT NO.
11. TITLE (Include Security Classification) Effect of Powder Characteristics on Microstructure and Properties in Alkoxide Prepared PZT Ceramics			
12. PERSONAL AUTHOR(S) R. C. Buchanan and J. Roy			
13a. TYPE OF REPORT Final	13b. TIME COVERED FROM 12/1/83 TO 11/30/84	14. DATE OF REPORT (Yr., Mo., Day)	15. PAGE COUNT
16. SUPPLEMENTARY NOTATION			
17. COSATI CODES		18. SUBJECT TERMS (Continue on reverse if necessary and identify by block number)	
FIELD	GROUP	SUB. GR.	PZT, coprecipitation parameters, dielectric properties, microstructure
19. ABSTRACT (Continue on reverse if necessary and identify by block number)			
SEE NEXT PAGE			
20. DISTRIBUTION/AVAILABILITY OF ABSTRACT UNCLASSIFIED/UNLIMITED <input checked="" type="checkbox"/> SAME AS RPT. <input type="checkbox"/> DTIC USERS <input type="checkbox"/>		21. ABSTRACT SECURITY CLASSIFICATION Unclassified	
22a. NAME OF RESPONSIBLE INDIVIDUAL		22b. TELEPHONE NUMBER (Include Area Code)	22c. OFFICE SYMBOL

ABSTRACT

SECURITY CLASSIFICATION OF THIS PAGE

Effects of coprecipitation parameters on agglomerate structure in PZT (53:47) powders prepared from butoxide precursors were studied. Results showed that differences in the agglomerate structures developed during coprecipitation persisted throughout the subsequent processing steps and the resulting sintered densities and microstructures to be correlated to the agglomerate structures. Coprecipitation parameters which most significantly affected the powder characteristics included temperature, dilution, pH, and hydrolysis rate (controlled by ^{water}H₂O concentration). Such processing parameters as powder rinsing, calcination temperature and spray-drying conditions also significantly influenced the developed microstructures. For equivalent processing conditions, most dense and uniform microstructures were developed with the softer (and smaller) agglomerate structures, achieved from an acid (pH 3.7) medium of low (3-5 vol%) solids content with rapid hydrolysis (~ 32 ml H₂O/min) and low temperature rise (10°C to 15°C). Measured dielectric constants (700-1000) on the sintered PZT samples were found to increase with average grain size which typically were larger for the basic (pH 11) powders.

Accession For	
NTIS GRA&I	<input checked="" type="checkbox"/>
DTIC TAB	<input type="checkbox"/>
Unannounced	<input type="checkbox"/>
Justification	
PER LETTER	
by	
Distribution/	
Availability Codes	

Dist	Avail and/or Special
A-1	



SECURITY CLASSIFICATION OF THIS PAGE

1. Introduction

Commercial PZT (Lead Zirconate Titanate) ceramic powders are typically formed from calcined mixtures of oxide or carbonate precursors. Difficulties with mixing often lead to incomplete reactions and localized inhomogeneities in the microstructure of the sintered ceramic. This condition in PZT contributes to a lack of reproducibility in the dielectric properties and aging characteristics and has the effect of limiting PZT use for many critical transducer applications. In consequence, alternate methods for powder preparation aimed at achieving intimate mixing by coprecipitation or by suspension of the oxide precursors in a finely dispersed and highly reactive state, have been investigated.

In preparing PZT ceramics, chemical coprecipitation from alkoxide precursors of Zr and Ti have been the most widely used of these alternate techniques. Difficulties with the use of Ti-nitrate and undesirable side effects with sulfate and chloride precursors make the alkoxide approach desirable. Brown and Mazdiyasi¹ used Zr and Ti alkoxide solutions blended with a solution of lead isoamyl oxide in distilled water to bring about decomposition and precipitation of the PZT phase. Excess lead oxide in the form of $Pb(OR'')_2$ was added to compensate for Pb loss during sintering. Calcination of the powder at $\sim 500^\circ C$ for 30-60 minutes produced the PZT phase.

Haertling and Land² prepared high-purity PLZT powders from materials consisting of lead oxide (PbO), lanthanum acetate ($La(AC)_3$), zirconium tetra-n-butoxide (ZNB) and titanium tetra-n-butoxide (TBT). The procedure consisted of weighing out the proper amounts of PbO and butoxides followed by blending in isopropyl alcohol. Lanthanum acetate solution was then added to the blending mixture which hydrolyzed the butoxides and produced a precipitate of mixed hydroxides, a process which was accelerated by the heat produced in the exothermic reactions.

Modifications to the basic alkoxide process aimed at producing

coprecipitated PZT and PLZT with different powder characteristics have been described by many authors.³⁻⁶ The coprecipitation process has also been used for adding minor ingredients to PZT compositions, either as sintering aids or for property control. Wittmer and Buchanan⁷ achieved significant reduction in the densification temperature of PZT (53:47) by incorporation of up to 1 wt% V_2O_5 during coprecipitation. The as-dried coprecipitated powders were found to be X-ray amorphous but powders calcined as low as 350°C produced XRD patterns characteristic of tetragonal PZT, with only slight lattice distortion. More recently, Tuttle⁸ coprecipitated powders of PSZT + Nb_2O_5 using a process similar to that employed by Wittmer and Buchanan.⁷ PbO , SnO_2 , and Nb_2O_5 were added to the blending mixture of TBT and ZNB. A 4:1 alcohol:water solution was used as the precipitating agent. Superior dielectric properties and high electrocaloric effects were obtained with the fired coprecipitated powders. Fired densities between 92.4% and 95.6% theoretical were obtained by firing at 1380°C using a standard double-crucible technique.

From the reported work it is evident that much sensitivity attaches to the alkoxide precipitation process, when such parameters as pH, dilution, dispersion, temperature and method of hydrolysis of the butoxide mixtures are considered since these parameters greatly affect agglomerate cohesion and size distribution in the precipitated powders.⁹ The effects of postprecipitation processing--washing, drying, calcination, dispersion, pressing--on powder characteristics and final densification have also been explored and were found to significantly influence the final densities and microstructures achieved.^{6,7,8}

The object of this study, therefore, was to investigate the relative influence of the coprecipitation and processing parameters on the powder characteristics, final densification, microstructure and dielectric properties of the sintered PZT ceramics.

11. Experimental

The PZT composition chosen for this study was $\text{Pb}(\text{Zr}_{0.53}\text{Ti}_{0.47})\text{O}_3$. This composition is near the morphotropic phase boundary for the PbZrO_3 - PbTiO_3 system and is known to give optimum permittivities and coupling coefficients.^{10,11} The powders were prepared by coprecipitation from starting high purity materials of electronic grade PbO (Hammond Lead Products, Inc., Hammond, Indiana), tetra-n-butyl titanate (E. I. duPont de Nemours Inc., Wilmington, Delaware), and zirconium tetra-n-butylate (Dynamite Nobel Co., Norwood, New Jersey).

Initially, a modified version of Wittmer's⁷ coprecipitation procedure was used. This procedure had only one blending step during coprecipitation and was termed the "single-step" process. It was modified such that the precipitated slurry was filtered in a Buchner funnel to speed dewatering and washing of the precipitate. The coprecipitation procedure consisted of: a) mixing the stoichiometric amounts of PbO , TBT, and ZNB (200 gm batch) in a blender at medium speed for about 15 min; b) adding a precipitating solution consisting of deionized water (30-100 vol%) in isopropanol (~ 250 ml of solution for a 200 g batch; pH of the solution was ~ 5.0); c) blending the thickened mixture for ~ 15 min until a smooth slurry was obtained; d) filtering the slurry using a Buchner funnel with solvent washing as appropriate; and e) drying the washed powder in a vacuum oven at 150°C for 4 h.

With this single-step blending, a significant rise in the temperature (85°C-95°C) and viscosity of the mixture was experienced, which made it difficult to maintain fluid mixing. To eliminate these problems, the process was further modified by diluting the batch with additional alcohol and using a two-step procedure which separated the coprecipitation and blending processes. This two-step coprecipitation procedure may be detailed as follows:

- a) To 200 ml of a 50/50 solution of isopropanol and n-butyl alcohol in a polyethylene beaker was added, while magnetically stirring, 85 ml of a mixture of Ti and Zr butoxides and PbO , calculated to give a 50 g batch of

(53:47) PZT composition. A wetting agent, Darvan C (~ 5 drops) was also added to aid dispersion;

- b) 200 ml of the water/isopropanol solution (to which glacial acetic acid or ammonium hydroxide was added for pH control) was added at 40-60 ml/min to cause precipitation of the mixed oxides;
- c) after stirring an additional 10 min, the precipitated mixture was transferred to a high-speed blender and blended for 15 min to produce a smooth, relatively stable slurry;
- d) the blended slurry was then directly spray-dried (using a laboratory spray-drier (Buchi Model 190--Brinkman Instrument Company) or else was washed and vacuum-dried as described.

Several parameters in the coprecipitation process for lead zirconate titanate prepared from the butoxide precursors, were investigated. These included the percentage of water, the rate of addition and the pH of the precipitating solution. Also investigated were the solids content of the PbO and Butoxide mixtures, the blending process, the temperature rise during coprecipitation, and the washing of the precipitate with different solvents. In evaluating the above parameters the following ranges were used: Concentration of suspended solids ranged from 2.0 to 7.0 vol%; water content of the precipitating water/alcohol solution varied from 25 to 100 vol% (12.5 to 49 vol% total liquid content) and was added at the rate of 6 to 60 ml/min. The pH range studied varied from 3.0 to 12.0 while the temperature rise during coprecipitation ranged from 10°C to 15°C (two-step blending) to 70°C for the single-step process. Where vacuum-drying was used, washing of the filtrate was carried out using deionized water, isopropanol, or a 60 vol% isopropanol mixture of the two solvents.

Calcination of the spray- or vacuum-dried precipitated powders was carried out in open platinum crucibles at 600°C to 850°C, to develop the PZT phase and promote grain growth. The calcined powder was milled for 5 h in polyethylene

Jars using ZrO_2 grinding media. A 60/40 vol% Isopropanol/water solution with Darvan C dispersant was found to be the most effective milling medium. A binder solution consisting of 1.0 wt% polyvinyl alcohol in water was added for the final hour of milling. The milled slurry was spray-dried and pellets ~ 1.6 cm dia. and 0.3 cm thick were uniaxially pressed at 207 MPa. The pressed pellets were sintered on Pt. foil supported on ZrO_2 setters at $1280^\circ C/4$ h using the standard double crucible technique of Okazaki, et al.,⁴ or in air at $950^\circ C/1$ h (for samples containing 0.5 wt% V_2O_5 as flux additive).⁷

The spray-dried, vacuum-dried and calcined powders as well as crushed sintered samples were analyzed by X-ray diffraction, using a Phillips Norelco diffractometer with filtered NiK_α radiation at 40 KV and 10 ma filament current, at a scanning rate of $1^\circ 2\theta$ /min. The powders were also subjected to DTA and TGA analysis using a (DuPont 1090) Thermal Analysis System. Particle size distribution measurements were made using an X-ray Sedigraph Analyzer (Micromeritics) and surface area measurements by a BET technique. SEM analysis on powders and sintered sections were made using an ISI-DS-130 Scanning Electron Microscope equipped with an energy dispersive X-ray analyzer. Sample densities were measured by water and mercury immersion techniques. Dielectric constant and dissipation factor measurements were made at 1.0 KHz using a capacitance bridge. Poling of the samples proved to be difficult with the smaller average grain sized samples.

III. Results and Discussion

Figure 1 shows SEM photomicrographs for the dried, as-precipitated powders prepared by the single- and two-step blending processes. Both powders were precipitated from acid medium of pH = 5. With the single step process (Fig. 1a), the morphology of the precipitated powders appeared to consist of hard, nearly dense agglomerates within the size range 2-5 μm . Reed, et al.,¹² differentiated between soft and hard agglomerates (aggregates), the latter being postulated to be held together by chemical or diffusion bonds, compared to soft

agglomerates which are believed to be bonded by Van der Waal's bonds or by magnetic forces. In contrast to the single-step process, powders prepared by the two-step blending (Fig. 1b) gave soft agglomerates in the size range 1-4 μm . These powders also showed a distinct subagglomerate structure with cluster sizes of $\sim 0.1 \mu\text{m}$. These differences are illustrated in Fig. 2, which shows agglomerate size distributions for the PZT coprecipitated powders as a function of pH and blending process. Significantly larger size distributions were measured with the single-step blending process at equivalent pH (8.5) confirming the trend noted in Fig. 1. Agglomerate size distributions also increased with pH for the same blending process.

The striking difference in morphology between the two powders in Figs. 1 and 2 can be attributed to the more highly dispersed state, greater fluidity and lower temperature of the two-step blending process. As indicated for the single-step process, there was difficulty in maintaining homogeneous mixing during coprecipitation due to gelation of the mixture and the high temperatures ($\sim 90^\circ\text{C}$) experienced during the hydrolysis reaction. With the diluted mixture used in the two-step process, the maximum temperature experienced was approximately 40°C . This lower temperature would be expected to slow the hydrolysis reaction,¹³ and as pointed out by Yoldas,¹⁴ dilution of the reacting species with neutral solvents also slows the reaction rate and enhances the uniformity of the hydrolysis reaction throughout the system. In contrast to the present finding where hard agglomerates were obtained at the higher precipitating temperatures (85°C to 95°C), work by van der Graaf et al.,¹⁵ found that ZrO_2 powders precipitated at room temperature yielded harder agglomerates than powders precipitated at higher temperatures ($\sim 100^\circ\text{C}$) which yielded the softer agglomerates.

The effect of water content and rate of addition on the amorphous character of the precipitated powders, as determined by X-ray diffraction analysis, is illustrated in Fig 3. Water contents of 33 vol% and 67 vol% in the

precipitating alcohol/water solutions were equivalent to 16 and 33 vol% of the total liquid content. Rates of water addition, as indicated, varied from 5.5 to 22 ml/min. The X-ray diffraction patterns for the dried precipitated powders were characterized by the presence of an amorphous hump, confirming the very small crystallite size of the powders and the absence of a clearly distinct PZT phase. Superimposed on the amorphous hump were crystalline diffraction peaks of unreacted PbO. The intensities of these peaks decreased with increasing hydrolysis (water content and addition rate), in line with the completely amorphous powders reported by Brown,¹ Haertling,¹⁶ and Wittmer.⁷ Calcination of the powders at 800°C/4 h gave only the PZT phase.

Harder and somewhat larger agglomerates were evident in the precipitates formed from low-water content solutions due to the higher temperatures experienced. Differences in the precipitated agglomerate structures were also retained throughout subsequent processing. This is illustrated in Fig. 4, where SEM fracture micrographs of calcined (800°C/4 h), pressed (207 MPa) but unfired samples are compared with fired (950°C/1 h), polished and thermally etched sections for powders precipitated with 25 and 67 vol% H₂O in the precipitating solution. The bimodal cluster and grain size distribution obtained with the 25 vol% H₂O solutions were in sharp contrast to the smaller clusters and uniform grain sizes obtained with the 67 vol% H₂O precipitate. These microstructures would not be predicted from the respective pressed (5.0 vs 4.4 g/cm³) and fired (7.5 vs 7.8 g/cm³) densities for the two powders (25 vol% vs 67 vol% H₂O). Coprecipitated powders sintered at 1280°C/4h (without V₂O₅ additions) showed essentially the same trends.

DTA heating and cooling curves for the water and/or alcohol rinsed coprecipitated powders are presented in Fig. 5. The DTA analyses showed exothermic reaction peaks occurring at approximately 200°C, 300°C, and 530°C. TGA analysis showed the first two peaks to be associated with weight losses, the maximum losses occurring near 300°C, and all weight loss occurring below

~ 400°C. The peaks were attributed respectively to loss of residual alcohol, elimination of the butoxide decomposition products, and to formation of the PZT phase. Rinsing with H₂O suppressed the exothermic peaks at ~ 200°C and 300°C. In contrast to rinsing with (isopropyl) alcohol which enhanced the lower peak and shifted the second peak to a higher temperature. With no rinsing of the precipitate the peak at 300°C was disproportionately larger, consistent with a higher content of organic residues.

In terms of densification, the H₂O rinsed powders gave significantly lower fired densities (~ 91% ThD) compared to the alcohol/water rinsed, (~ 96% of ThD.), with isopropanol washed samples intermediate at 95% ThD. The base density for PZT (53:47) was taken as 8.0 g/cm³. These observations are consistent with fired densities obtained by Haberkorn¹⁷ on water and alcohol washed stabilized ZrO₂ powders. The differences were attributed to the weaker bonded agglomerates formed with alcohol washed powders as a result of reduced surface ionic absorption.

Figure 6 shows the effect of pH on the agglomerate structure of the "as-precipitated" powders following initial spray drying. The acid powder (pH 3.7) had an average agglomerate size of ~ 5 μm with a well-defined subagglomerate structure. In contrast, the basic powder (pH 11) had an average agglomerate size of ~ 10 μm, appeared harder and had a less distinct substructure. The increase in the agglomerate size for the basic powders was confirmed by the Sedigraph analysis shown in Fig. 7. The powders precipitated by the pH 3 solution had an average agglomerate size of ~ 0.5 μm, which increased to ~ 0.9 μm for the pH 10 solution with a narrower size distribution. The difference in average size distribution between the SEM and sedigraph data was due to the partial breakup of the spray-dried agglomerates by addition of a deflocculant and by mechanical dispersion during the Sedigraph tests.

Figure 8 shows SEM fracture micrographs for sintered ($1280^{\circ}\text{C}/4\text{ h}$) samples of the two powders discussed in Fig. 6. The pH 3.7 powders, which had a uniform pressed microstructure, yielded a very dense microstructure and smaller average grain size ($\sim 10\text{ }\mu\text{m}$) than the pH 11 sample ($\sim 20\text{ }\mu\text{m}$ avg GS). Both samples were calcined at $800^{\circ}\text{C}/4\text{ h}$, which throughout this study generally resulted in larger grain sizes for the basic powders. The grain size disparity was in line with the size disparity and hardness of the agglomerated structures formed during coprecipitation of the powders. Transgranular and intergranular cracks were observed, particularly for the larger grain sized sample due in part to microcracks introduced by quenching to prevent accumulation of liquid phase on the sample surface.

BET surface areas determined for the two powders were $132\text{ m}^2/\text{g}$ (pH = 3.7) and $128\text{ m}^2/\text{g}$ (pH = 11) compared to the $26\text{ m}^2/\text{g}$ reported by Biggers et al.,⁶ for PZT powders precipitated from aqueous medium. This difference reflects the more highly dispersed conditions prevailing during the coprecipitation process. The large surface area also reflected the very small crystallite sizes (~ 150 to 200 \AA) of the precipitated powders. The pH, therefore, did not greatly affect crystallite size formation, rather it affected agglomeration tendency and bonding within the structures formed.

This difference in agglomeration tendency caused marked differences in powder morphology on calcination. Figure 9 shows SEM fracture micrographs of calcined powders following spray-drying, a second milling and pressing at 207 MPa. For the powders calcined at $800^{\circ}\text{C}/4\text{ h}$, (Figs. 9a,b), the aggregates for the pH 3.7 powders were readily broken up after milling but were solidified or essentially sintered for pH 11 powders, indicating the formation of much harder agglomerates in the basic powder during coprecipitation. In general, powders calcined at $750^{\circ}\text{C}/4\text{ h}$ (Figs. 9c,d) gave smaller and more uniform aggregate sizes but always larger for the basic powders.

Figure 10 shows SEM fracture micrographs of the sintered ($950^{\circ}\text{C}/4\text{ h}$) samples for the pH and calcination conditions detailed in Fig. 9. The effect of pH and calcination conditions on for the pressed and fired densities are shown in Fig. 11. Densities obtained for the pH 3.7 and pH 11 powders were similar for equivalent calcination and sintering conditions, but were lower for other pH values. Powders calcined at $750^{\circ}\text{C}/4\text{ h}$ gave highest densities for both pH conditions.

The existence of density maxima at pH 3.7 and pH 11.0 in the densification curves coincides with the observed stability maxima, as a function of pH, for colloidal suspensions of oxide materials such as SiO_2 . At the lower pH values (2.5 to 3.5) the particles have very little ionic charge and stability is maintained by a hydration layer surrounding each particle rather than by electrostatic repulsion. Dried sols of such acid pH powders, therefore, tend to be bonded by Van der Waals forces and, in consequence, are softer and less agglomerated. In contrast, in the pH range 10 to 11 electrolyte presence causes development of net charges on the particle surfaces and stability is maintained by electrostatic repulsion. Dried sols of high pH, therefore, tend to be more strongly bonded, resulting in larger and harder agglomerate structures. These observations are in keeping with the observed agglomerated states as a function of pH for the precipitated PZT powders, and suggest a state of maximum dispersion for the pH 3.7 and pH 11 suspensions. This in turn would lead to higher packing and sintered densities, and to the marked differences in the grain size and microstructures noted.

The average grain size for the powders calcined at 800°C increased, following sintering at $950^{\circ}/1\text{ h}$, from 0.3 μm to 1.0 μm for the pH 3.7 powders (Figs. 9 and 10) and from 1.0 μm to 1.7 μm for the pH 11 powders. For the powders calcined at 750°C , the average grain size increased from 0.25 μm to 2.5 μm for the pH 3.7 powder, and from 0.5 μm to 1.0 μm for the pH 11 powder.

The data show densification and grain growth rates to be significantly enhanced for the lower temperature (750°C/4 h vs 800°C/4 h) calcined powders, reflecting the higher driving force for densification with the smaller sized aggregates with the liquid phase assisted sintering. Grain sizes and final microstructures developed were much influenced by the calcination conditions, reported also by Venkatarami and Biggers,¹⁸ but significantly also by the powder morphology developed, as a function of pH, during coprecipitation from the alkoxide precursor mixtures. With close control of the coprecipitation parameters (especially pH) combined with manipulation of the calcination conditions, therefore, controlled microstructures in the sintered PZT can be achieved (at least under conditions of low temperature liquid phase assisted sintering) which would lead to improved reproducibility of dielectric properties and aging characteristics.

Table 1 gives grain size and dielectric property data for the samples shown in Fig. 10 with sintered densities $\geq 95\%$ theoretical density. Measured dissipation factors were $< 2.0\%$ and dielectric constants were in the range 700 to 1000 at 25°C, in line with reported values for PZT.¹⁹ The increase in dielectric constant noted with grain size is similar to that reported by Okazaki²⁰ for small grain size ($< 4 \mu\text{m}$) PLZT samples. The observed increase in dielectric constant with grain size can be attributed to a volume decrease in the more insulating boundary phase as well as to a measured increased conduction and the ease of polarization of the larger grains. This is further illustrated in Fig. 12 which compares the dielectric constant as a function temperature for the non-fluxed PZT samples in Fig. 8 (sintered at 1280°C/4 h) for pH conditions 3.7 and 11.0. These samples showed a marked increase in dielectric constant with average grain size in the range 10-20 μm . This is in contrast to the reported decrease in dielectric constant with grain size by Webster²¹ and also by Haertling.¹⁶ For both samples in Fig. 12, loss tangents up to $\sim 200^\circ\text{C}$ were

below 2.0% but increased sharply on approach to the Curie points ($\sim 394^{\circ}\text{C}$). The dielectric constants also increased almost linearly up $\sim 250^{\circ}\text{C}$ and attained values $> 10,000$ at the Curie points. The marked differences in dielectric constants between the two powders indicated the sensitivity of the final microstructure and properties to initial powder characteristics.

IV. Conclusions

1. This study has shown that in the coprecipitation of PZT from butoxide precursors such powder characteristics as amorphous structure, agglomerate cohesion (hardness) and size distribution were established during the coprecipitation process. Differences at this level tended to persist throughout subsequent processing resulting in significantly different microstructure and properties.
2. The parameters which most sensitively affected coprecipitation, were found to be dilution, pH, temperature, and precipitation or hydrolysis rate (controlled by H_2O addition). Low solids constant ($\sim 3\text{-}5$ vol% PbO), low temperature rise ($< 15^{\circ}\text{C}$), acidic pH ($\sim 3\text{-}4$) and high precipitation rates (25 to 32 ml $\text{H}_2\text{O}/\text{min}$) were found to promote smaller and more uniformly sized agglomerates. These conditions were readily achieved in the two-step blending process described.
3. Both as a milling and washing medium, isopropanol/water solution (60/40 vol%) was found to promote higher fired densities and more uniform microstructures.
4. Calcination temperature and spray-drying of dispersed powders were found to be important processing variables. Lower calcination temperatures were required with the basic powders to achieve equivalent microstructures.
5. Grain sizes and dielectric constants obtained with the basic (pH 11) powders more generally larger particularly at the higher (800°C) calcination temperatures.

V. Acknowledgements

This work was supported by the Office of Naval Research under contract US Navy N00014-80-K-0969 and in part by the National Science Foundation under MRL grant no. DMR-80-20250, and is gratefully acknowledged.

VI. References

1. L. M. Brown and K. S. Mazdiyani, "Cold-Pressing and Low-Temperature Sintering of Alkyoxy-Derived PLZT," J. Am. Ceram. Soc., 55 541-555 (1972).
2. G. Haertling and C. Land, "Recent Improvements in the Optical and Electrooptic Properties of PLZT Ceramics," Ferroelectrics, 3 269-280 (1972).
3. M. Murata, K. Wakino, K. Tanaka, and Y. Hamakawa, "Chemical Preparation of PLZT Powder from Aqueous Solution," Mat. Res. Bull., 11 323-328 (1976).
4. K. Okazaki, "Developments in Fabrications of Piezoelectric Ceramics," Ferroelectrics, 41 77-96 (1982).
5. R. Brooks and D. K. Murphy, "Production Scale PLZT Powder Preparation," Ferroelectrics, 27 179 (1980).
6. J. V. Bigger and S. Venkataramani, "Preparations and Reactivity of Lead Zirconate-Lead Titanate Solid Solutions Produced by Precipitation from Aqueous Solutions," Mat. Res. Bull., 13 717-727 (1978).
7. D. E. Wittmer and R. C. Buchanan, "Low-Temperature Densification of PZT with Vanadium Pentoxide Additive," J. Am. Ceram. Soc., 64 485-490 (1981).
8. B. A. Tuttle, "Polarization Reversal and Electrocaloric Measurements for Field-Enforced Transitions in the System Lead Zirconate-Lead Titanate-Lead Oxide-Tin Oxide," Ph.D. Thesis, University of Illinois at Urbana-Champaign, (1981).
9. T. B. Weston, "Studies in the Preparation and Properties of Lead-Zirconate Lead Titanate Ceramics," J. Can. Ceram. Soc., 32 100-115 (1963).

10. L. E. Cross, and K. H. Haerdtl, "Ferroelectrics," Encyclopedia of Chemical Technology, 10, pp. 1-30, John Wiley and Sons, Inc., New York, NY (1980).
11. Ya. S. Bogdanov, A. Ya Dantsiger, V. F. Zhestkov, et al., "Changes in the Dielectric Constant in the Tetragonal Rhombohedral Transition Region in the System Based on PZT," Izv. Akad. Nauk. SSSR, Neorg. Mater., 16 [6] 1048-1050 (1980) (Russ.).
12. J. S. Reed, T. Carbone, C. Scott, and S. Lukasiewicz, "Some Effects of Aggregates and Agglomerates in the Fabrication of Fine Grain Ceramics," Processing of Crystalline Ceramics: Materials Sciences Research, Vol 11, pp. 171-180, Plenum Press, New York (1978).
13. Takashi Yamaguchi, S. H. Cho, and M. Hakomori, et al., "Effects of Raw Materials and Mixing Methods on the Solid State Reactions Involved in Fabrication of Electronic Ceramics (PZT)," Ceramurgia Int., 2 [2] 76-80 (1976) (in Eng.).
14. B. E. Yoldas, "Effect of Variation in Polymerized Oxides on Sintering and Crystalline Transformation," J. Am. Ceram. Soc., 65 [8] 387-393 (1982).
15. M. A. C. G. van der Graaf, K. Keizer, and A. J. Burggrof, "Influence of Agglomerate Structures in Ultra Fine Substituted Zirconia Powders on Compaction and Sintering Behavior," pp. 88-92 in Science of Ceramics, Vol. 10. Edited by E. Hausner. Deutsche Keramische Gesellschaft, 1980.
16. G. H. Haertling, "Improved Hot-Pressed Electrooptic Ceramics In (Pb,La)(Zr,Ti)O₃ System," J. Am. Ceram. Soc., 54 [6] 303-309 (1971).
17. K. Haberko, "Characteristics and Sintering Behaviour of Zirconia Ultrafine Powders," Ceramurgia Int'l., 5 148-154 (1979).
18. S. Venkataramani and J. V. Biggers, "Reactivity of Zirconia in Calcining of Lead Zirconate-Lead Titanate Compositions Prepared from Mixed Oxides," Ceram Bull., 59 462-466 (1980).

19. Z. Wrobel and Cz. Kus, "Electric Properties in Solid Solutions of PZT Near the Morphotropic Phase Boundary," Ferroelectrics, 22 [1-2] 801-803 (1978).
20. Kayoshi Okazaki and Kunkiro Nagata, "Relation Between Grain Density and Size and the Piezoelectric Properties of Ceramics Based on Pb, Zr, and Ti," Ceram. Inf. (Faenza), 12 [4] 173-178 (1977).
21. A. H. Webster, T. B. Weston, and R. R. Craig, "Some Ceramic and Electrical Properties of Bodies Fabricated from Coprecipitated Lead-Zirconate-Titanate Hydroxide," J. Can. Ceram. Soc., 34 121-136 (1965).

TABLE I
EFFECT OF pH AND CALCINATION TEMPERATURE ON
GRAIN SIZE AND DIELECTRIC PROPERTIES OF PZT

pH	CALCINATION (temp./time)	GRAIN SIZE (μm)	DIELECTRIC CONSTANT	% DISP. FACTOR
3.7	800°C/4 h	1.0	760	1.2
11.0	800°C/4 h	1.5	880	1.0
3.7	750°C/4 h	2.5	930	1.1
11.0	750°C/4 h	1.0	700	2.0

Sintering temp: 950°C/1 h. Dielectric data at 25°C.

LIST OF FIGURES

- Figure 1. SEM micrographs of "as-precipitated" powders comparing precipitating procedures: a) one-step, b) two-step blending processes.
- Figure 2. X-ray Sedigraph plot of agglomerate size distribution for coprecipitated PZT powders as a function of pH and blending process.
- Figure 3. X-ray diffraction patterns showing decrease in unreacted PbO content of "as-precipitated" PZT powder with increasing H₂O content and faster addition rate of the precipitating solution.
- Figure 4. SEM photomicrographs of fracture surfaces of unfired PZT (single-step process) samples from precipitating solutions containing: a) 25 vol% H₂O; b) 67 wt% H₂O (pH 5); c) fired (950°C/1 h), polished and thermally etched photomicrographs of a) and b) shown in c) and d) respectively.
- Figure 5. Differential thermal analysis curves comparing washing media: isopropanol, water and isopropanol/water solution.
- Figure 6. SEM photomicrographs of precipitated powders following drying for precipitation conditions of: a) pH 3.7, b) pH 11.
- Figure 7. Agglomerate size distribution of precipitated PZT powders showing effect of pH on equivalent spherical diameters.
- Figure 8. SEM photomicrographs of fracture surfaces of fired (1280°C/4 h) PZT for the precipitation conditions: a) pH 3.7, b) pH 11, both calcined at 800°C/4 h.
- Figure 9. SEM photomicrographs of fracture surfaces of unfired PZT obtained for precipitation and calcination conditions: a) pH 3.7, calcined 800°C/4 h; b) pH 11, calcined 800°C/4 h; c) pH 3.7, calcined 750°C/4 h; d) pH 11, calcined 750°C/4 h.

Figure 10. SEM photomicrographs of fracture surfaces of fired ($950^{\circ}\text{C}/1\text{ h}$) PZT + 0.25 wt% V_2O_5 obtained for precipitation and calcination conditions in Fig. 9: a) pH 3.7, calcined $800^{\circ}\text{C}/4\text{ h}$; b) pH 11, calcined $800^{\circ}\text{C}/4\text{ h}$; c) pH 3.7, calcined $750^{\circ}\text{C}/4\text{ h}$; d) pH 11, calcined $750^{\circ}\text{C}/4\text{ h}$.

Figure 11. Effect of pH of precipitating solution on the pressed and fired densities ($950^{\circ}\text{C}/1\text{ h}$) of PZT (+ 0.25 wt% V_2O_5).

Figure 12. Plot of dielectric constant and $\tan \delta$ for sintered ($1280^{\circ}\text{C}/4\text{ h}$) coprecipitated PZT powders in Fig. 8 showing effect of pH and grain size.

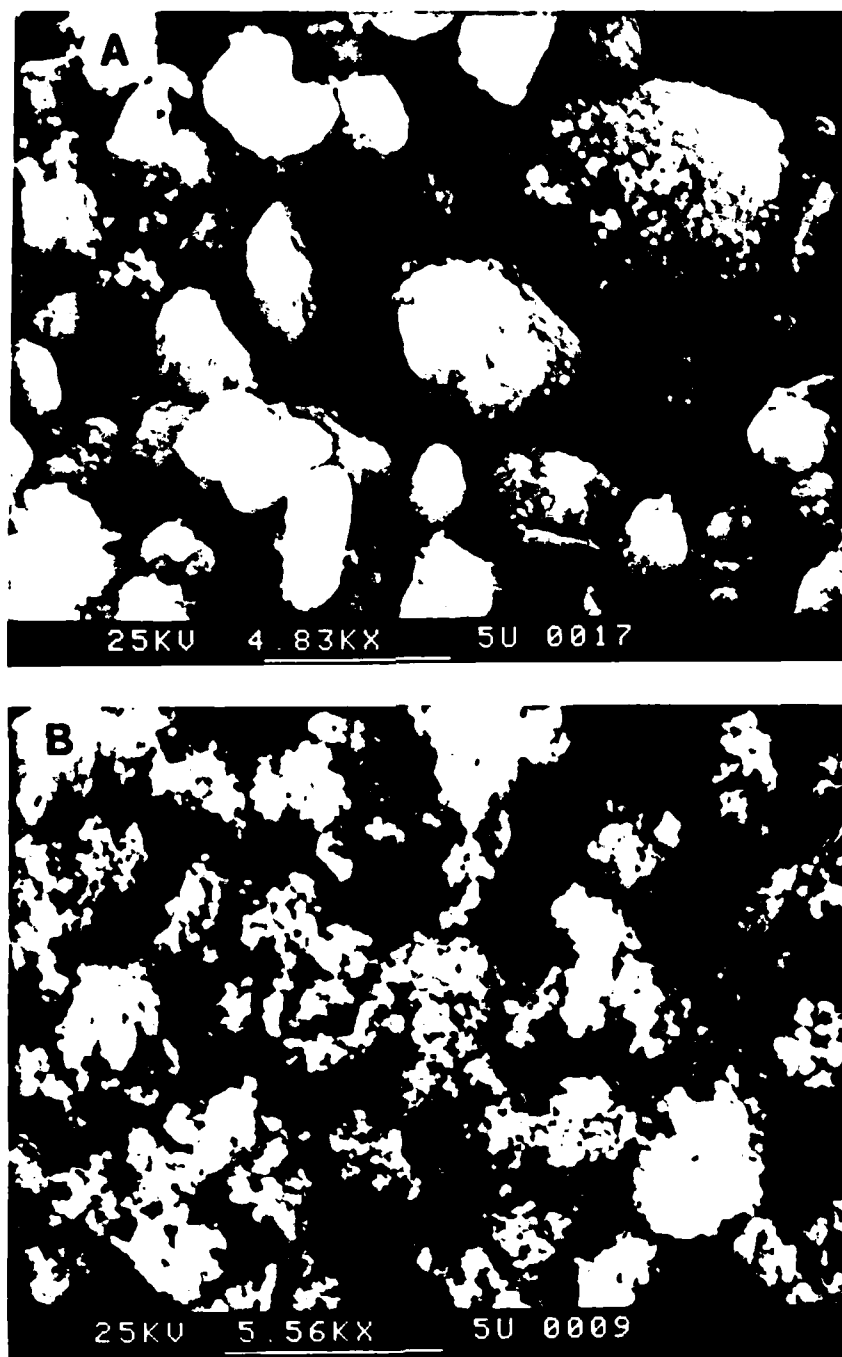


Figure 1. SEM micrographs of "as-precipitated" powders comparing precipitating procedures: a) one-step, b) two-step blending processes.

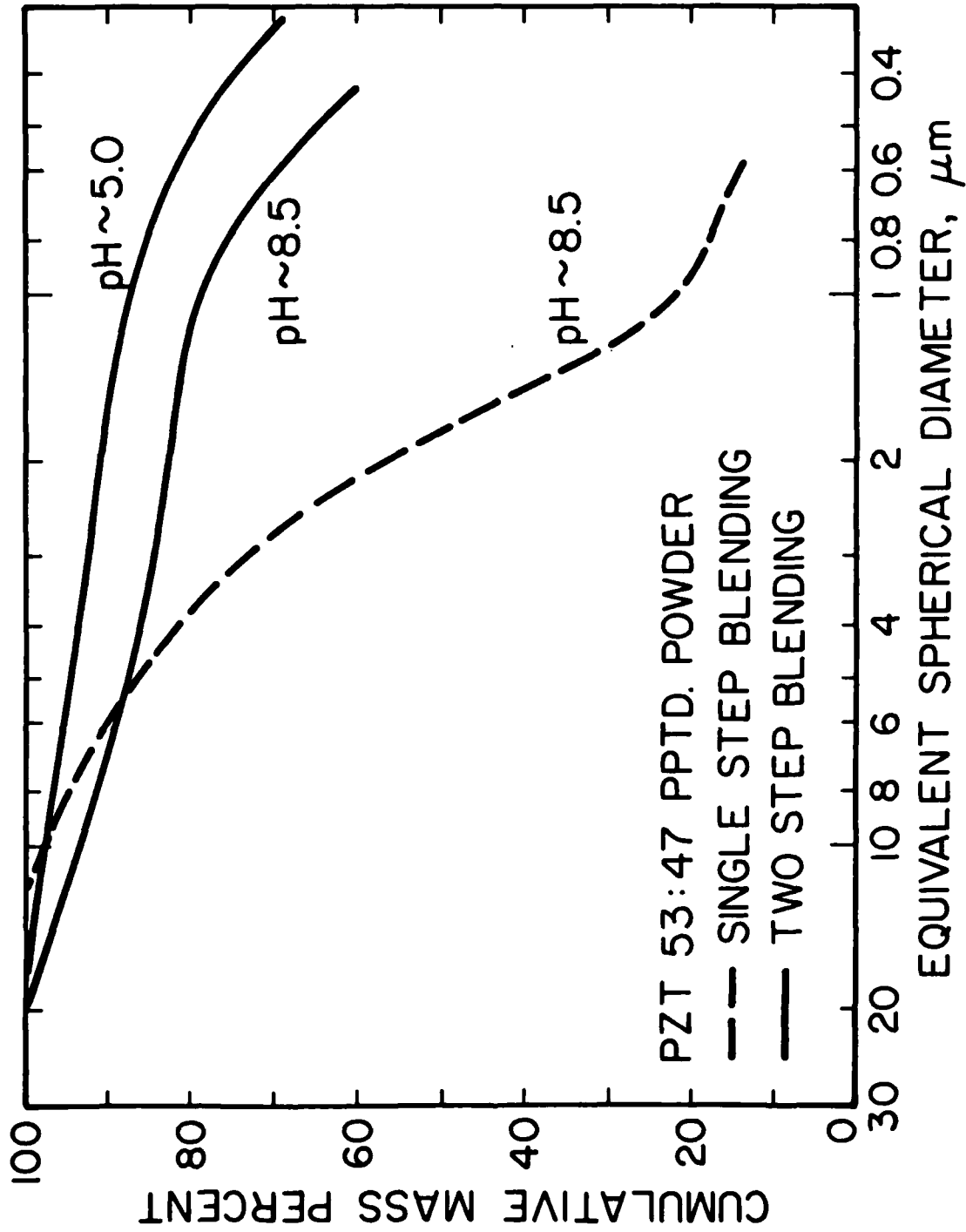


Figure 2. X-ray Sedigraph plot of agglomerate size distribution for coprecipitated PZT powders as a function of pH and blending process.

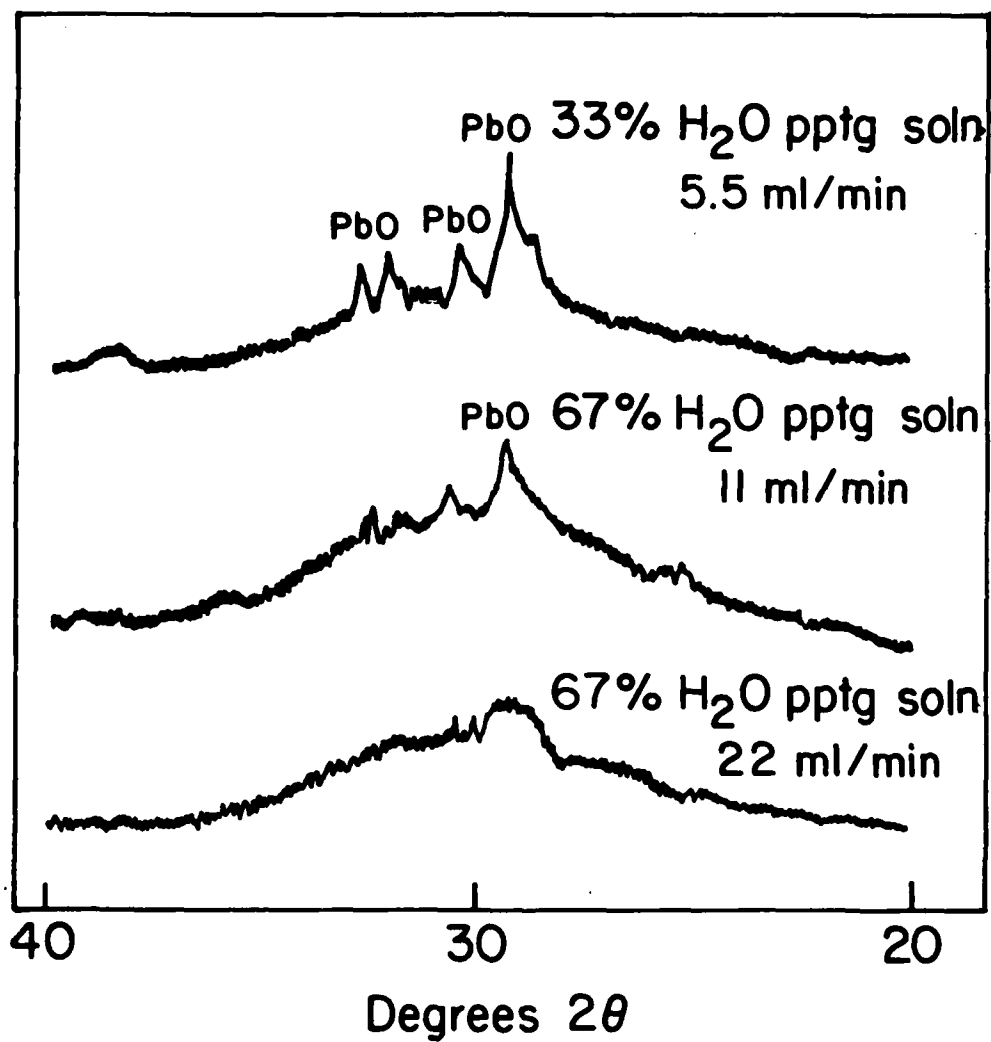


Figure 3. X-ray diffraction patterns showing decrease in unreacted PbO content of "as-precipitated" PZT powder with increasing H₂O content and faster addition rate of the precipitating solution.

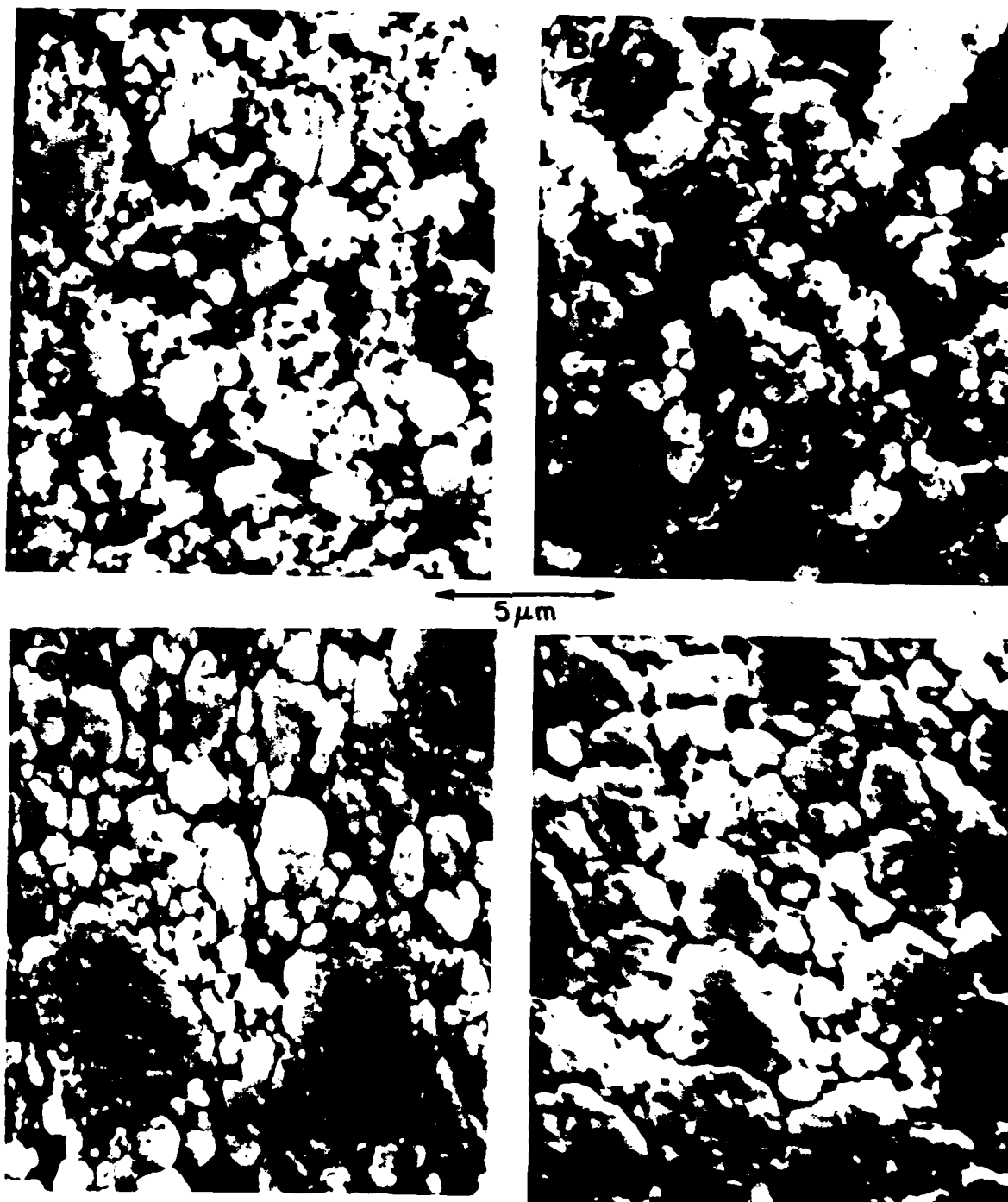


Figure 4. SEM photomicrographs of fracture surfaces of unfired PZT (single-step process) samples from precipitating solutions containing: a) 25 vol% H_2O ; b) 67 wt% H_2O (pH 5); c) fired ($950^{\circ}C/1$ h), polished and thermally etched photomicrographs of a) and b) shown in c) and d) respectively.

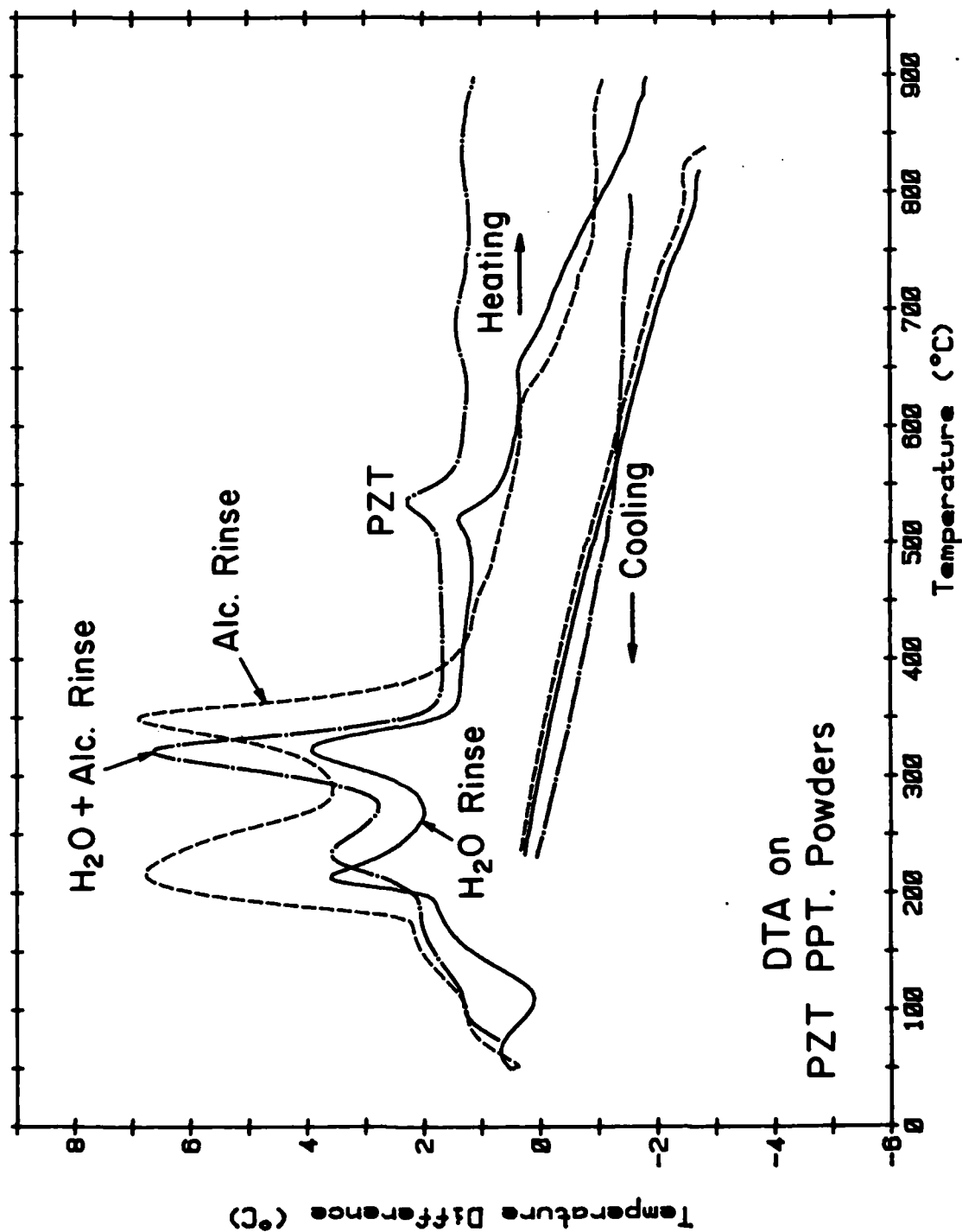


Figure 5. Differential thermal analysis curves comparing washing media: isopropanol, water and isopropanol/water solution.

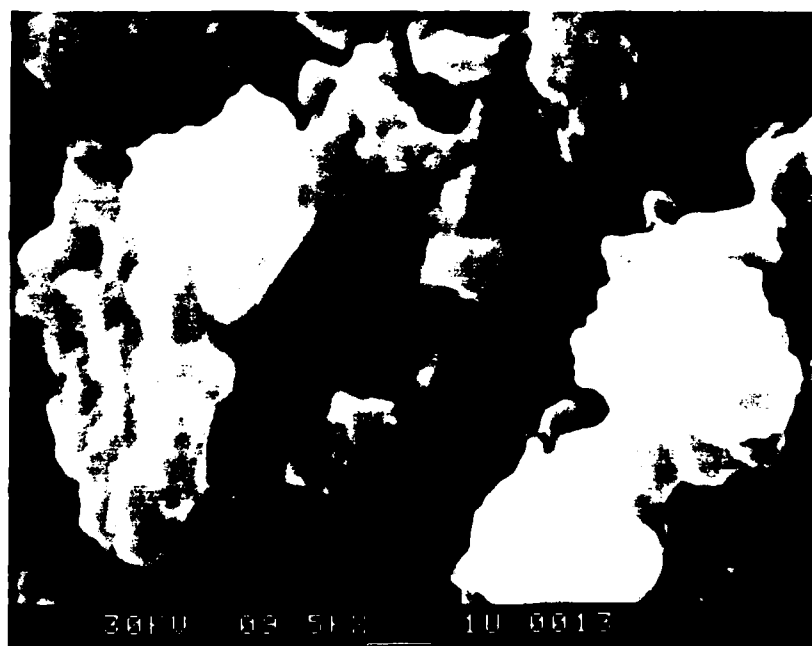
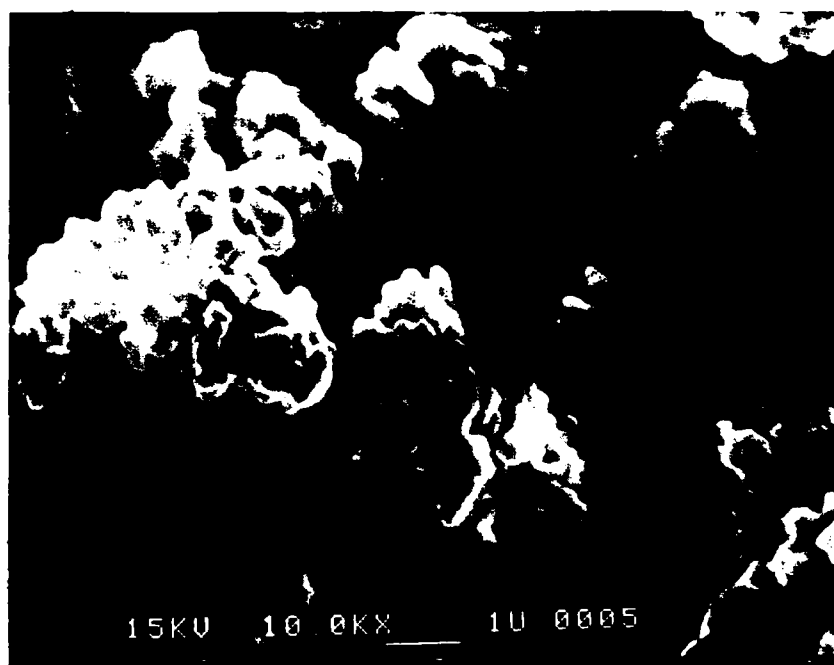


Figure 6. SEM photomicrographs of precipitated powders following drying for precipitation conditions of: a) pH 3.7, b) pH 11.

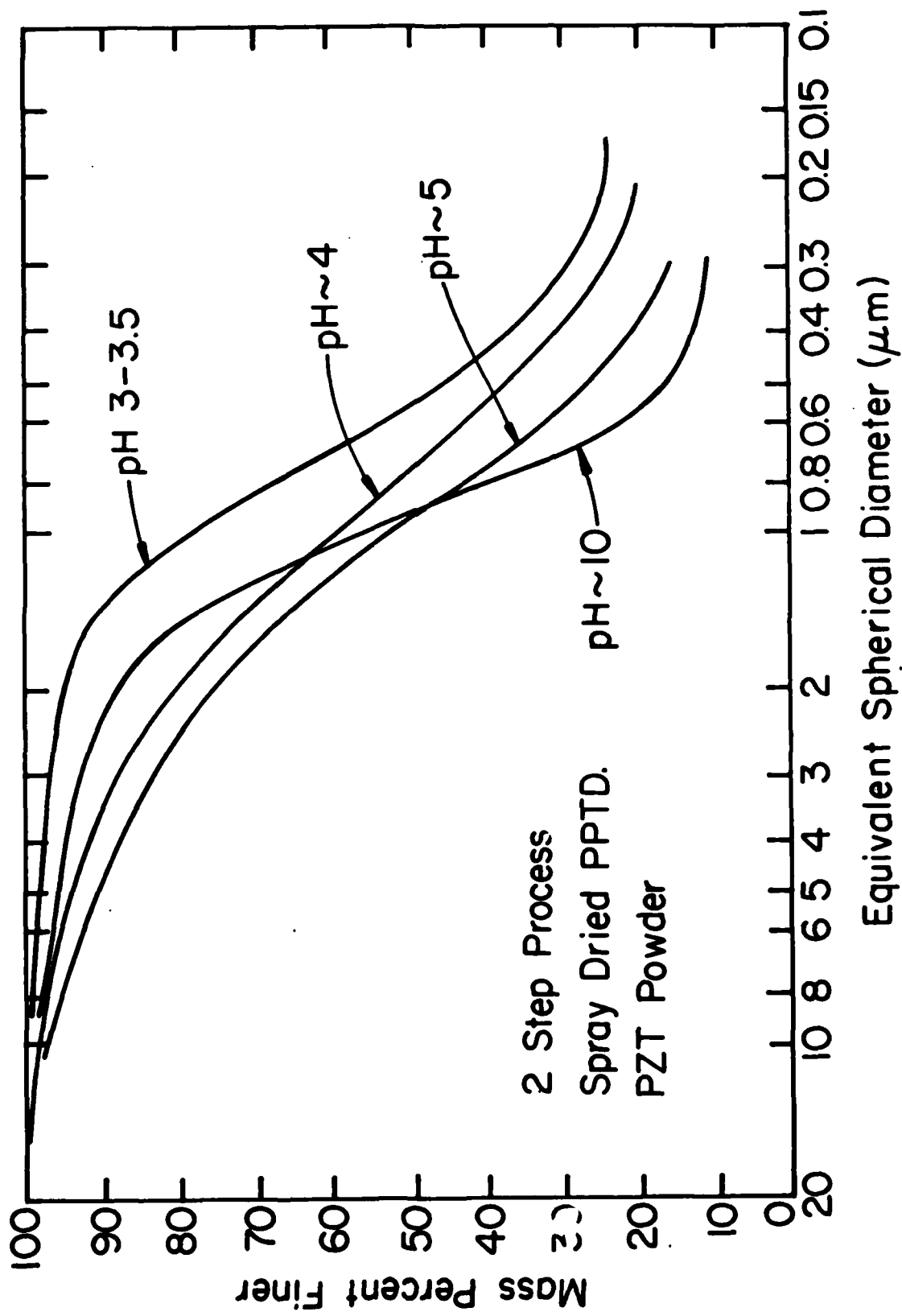


Figure 7. Agglomerate size distribution of precipitated PZT powders showing effect of pH on equivalent spherical diameters.

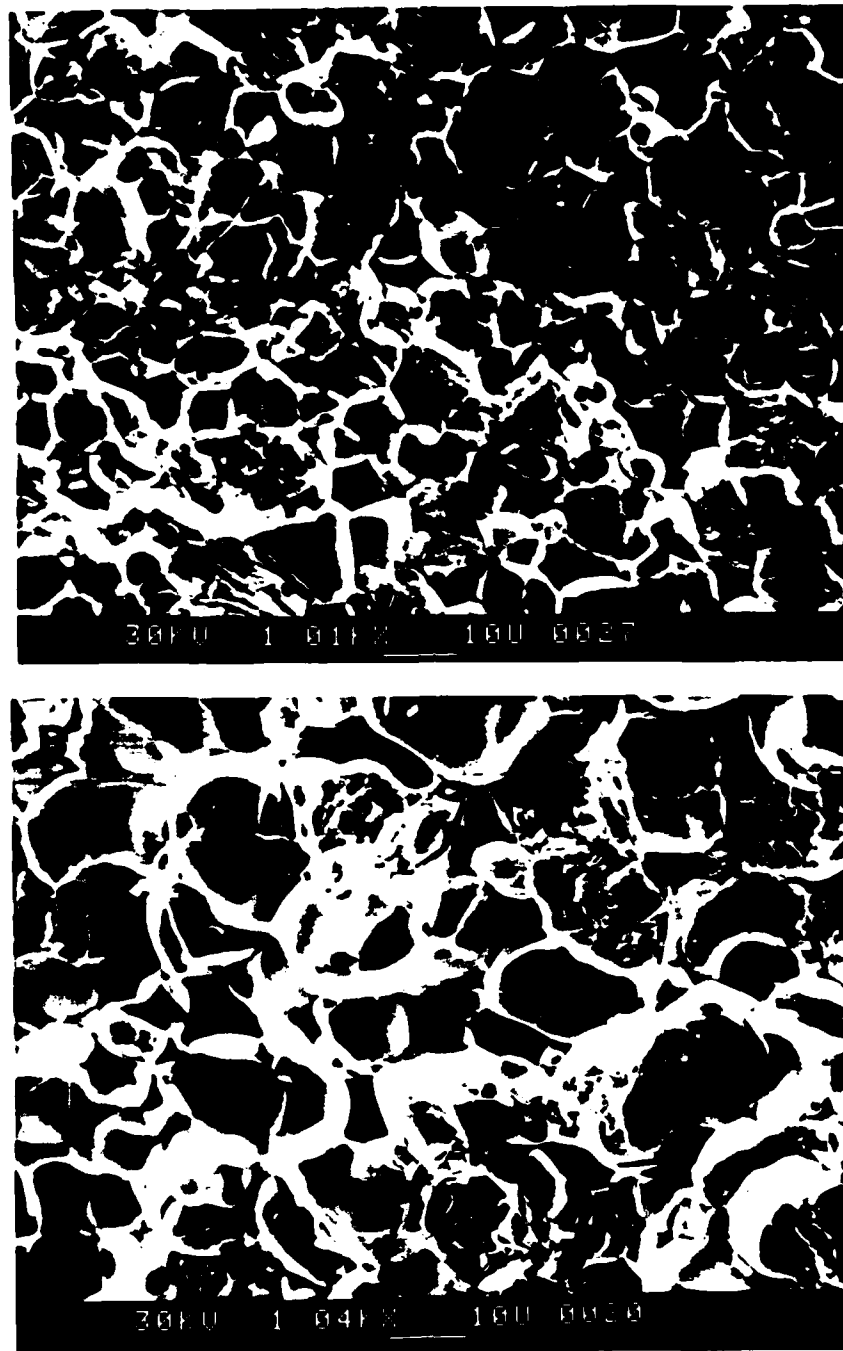


Figure 8. SEM photomicrographs of fracture surfaces of fired ($1280^{\circ}\text{C}/4\text{ h}$) PZT for the precipitation conditions: a) pH 3.7, b) pH 11, both calcined at $800^{\circ}\text{C}/4\text{ h}$.

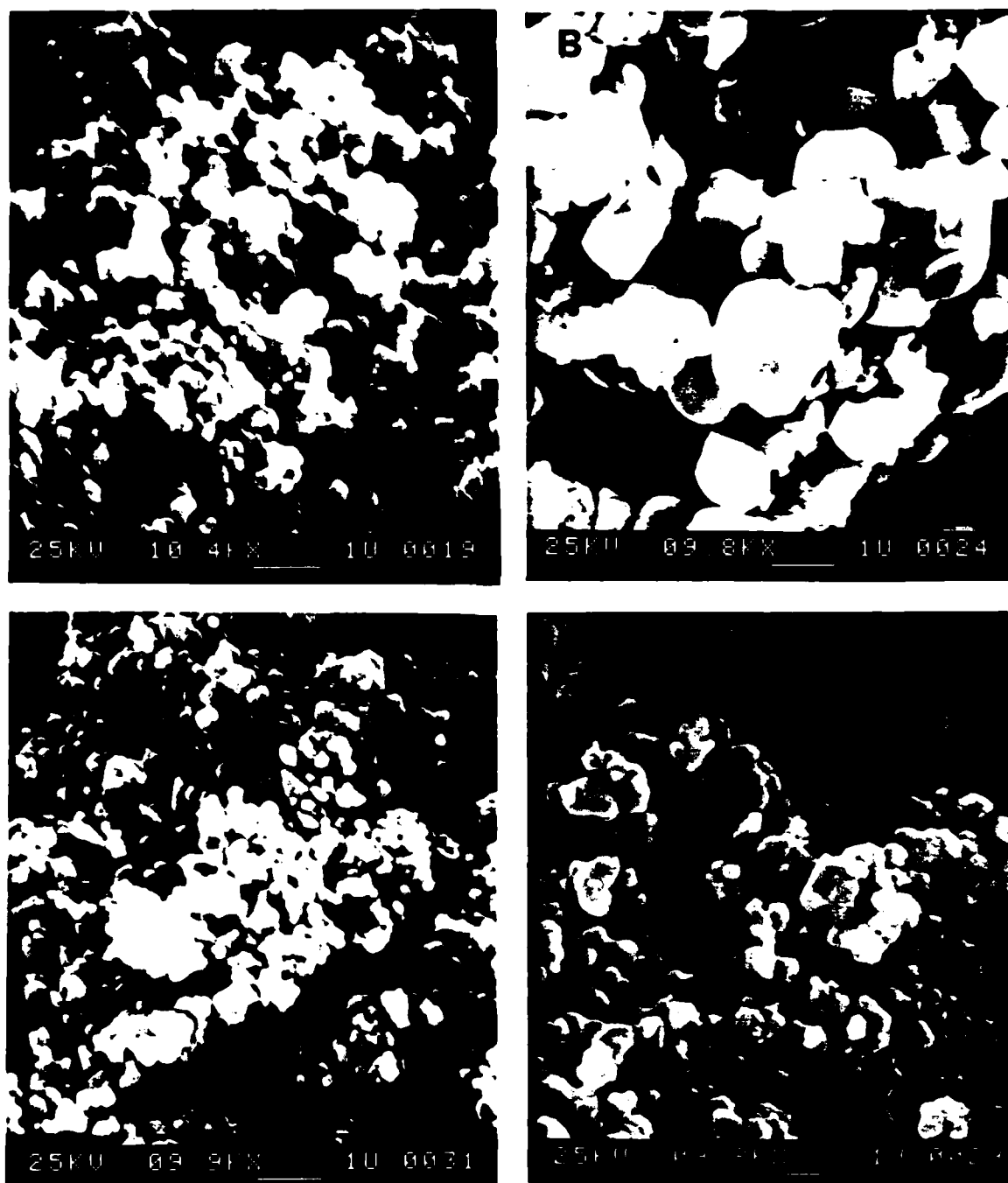


Figure 9. SEM photomicrographs of fracture surfaces of unfired PZT obtained for precipitation and calcination conditions: a) pH 3.7, calcined $800^{\circ}\text{C}/4\text{ h}$; b) pH 11, calcined $800^{\circ}\text{C}/4\text{ h}$; c) pH 3.7, calcined $750^{\circ}\text{C}/4\text{ h}$; d) pH 11, calcined $750^{\circ}\text{C}/4\text{ h}$.

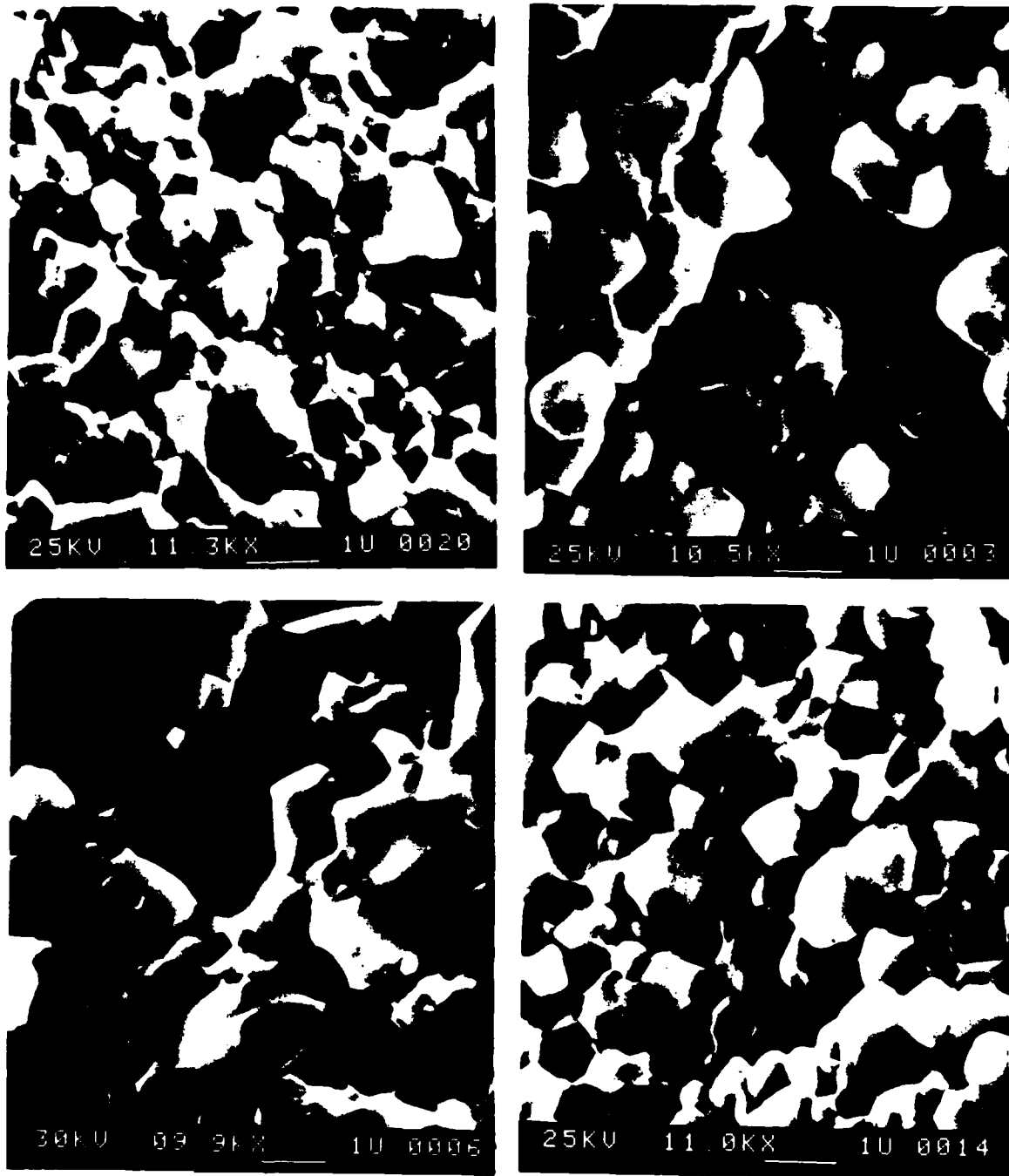


Figure 10. SEM photomicrographs of fracture surfaces of fired ($950^{\circ}\text{C}/1\text{ h}$) PZT + 0.25 wt% V_2O_5 obtained for precipitation and calcination conditions in Fig. 9: a) pH 3.7, calcined $800^{\circ}\text{C}/4\text{ h}$; b) pH 11, calcined $800^{\circ}\text{C}/4\text{ h}$; c) pH 3.7, calcined $750^{\circ}\text{C}/4\text{ h}$; d) pH 11, calcined $750^{\circ}\text{C}/4\text{ h}$.

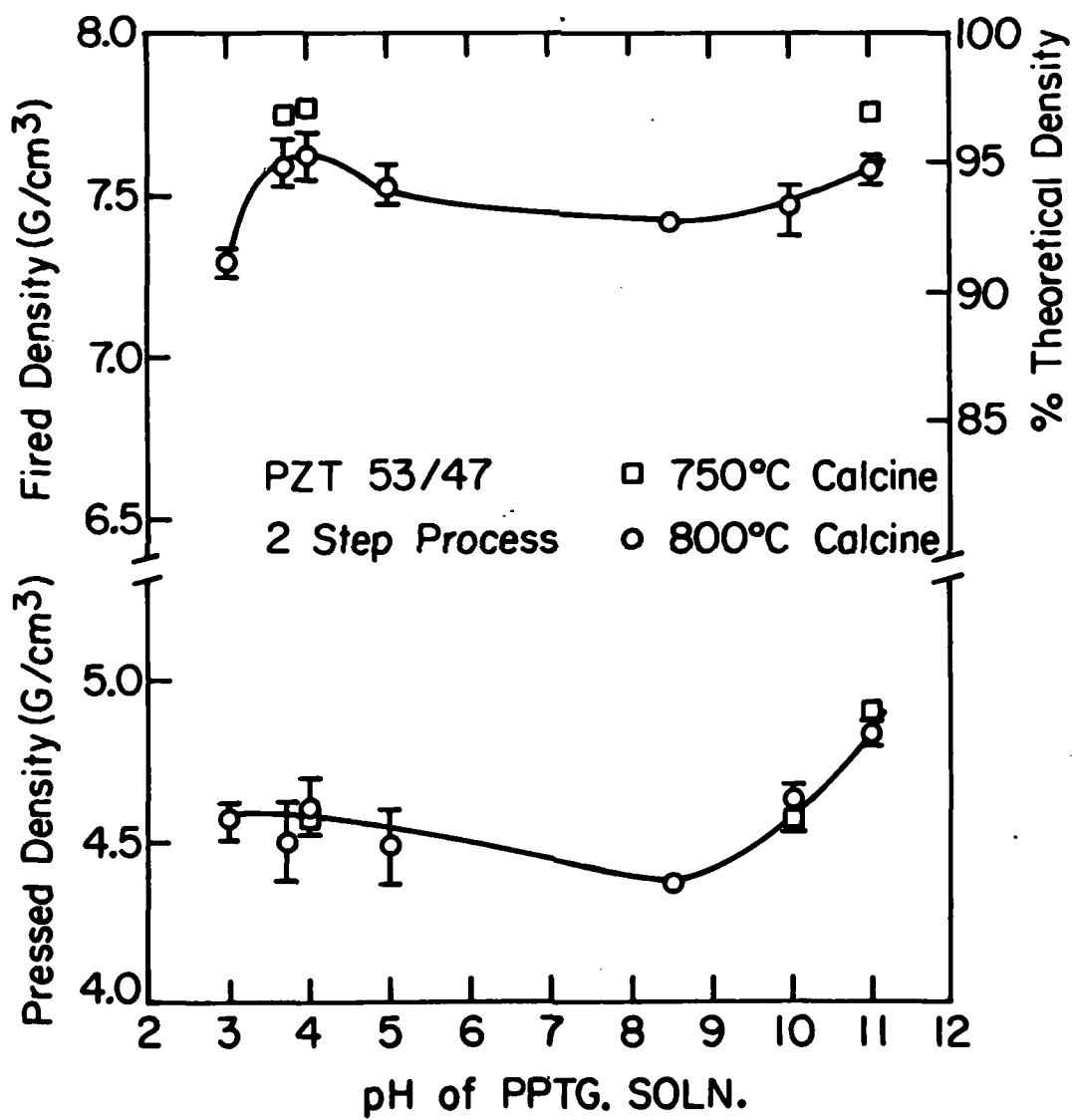


Figure 11. Effect of pH of precipitating solution on the pressed and fired densities (950°C/1 h) of PZT (+ 0.25 wt% V₂O₅).

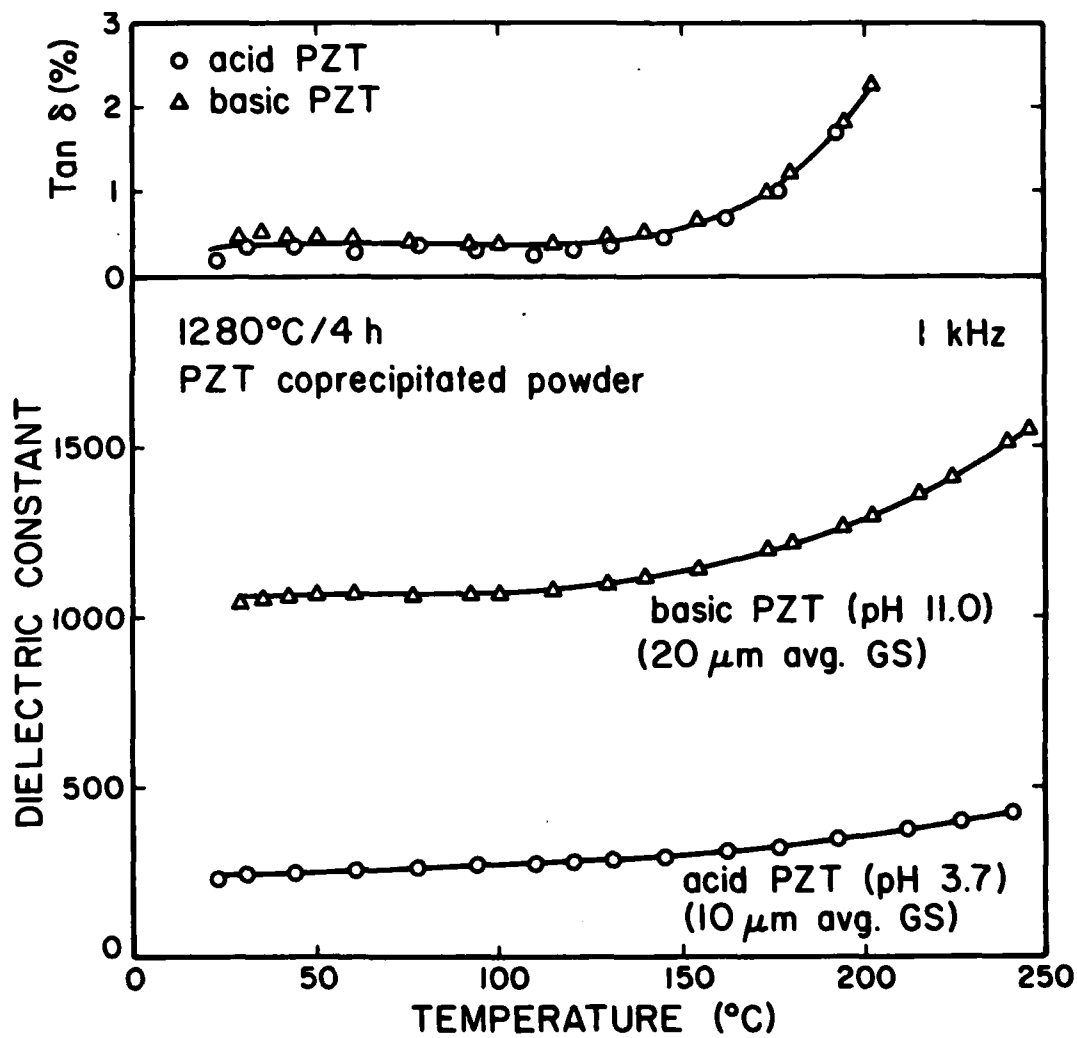


Figure 12. Plot of dielectric constant and $\tan \delta$ for sintered (1280°C/4 h) coprecipitated PZT powders in Fig. 8 showing effect of pH and grain size.

Summary of Work Accomplished
Under Contract No. US NAVY-N-00014-80-K-0969

Reports

Reports issued under this contract include the following:

1. R. C. Buchanan and S. Pope, "Optical and Electrical Properties of Yttria Stabilized Zirconia (YSZ) Crystals," (ONR Report #5), University of Illinois at Urbana-Champaign, Department of Ceramic Engineering, Urbana, IL 61801 (September, 1981).
2. R. C. Buchanan and J. Boy, "Effect of Coprecipitation Parameters on Powder Characteristics and On Densification of PZT Ceramics," (ONR Report #6), University of Illinois at Urbana-Champaign, Department of Ceramic Engineering, Urbana, IL (September 1982).
3. R. C. Buchanan and D. M. Wilson, "Densification of Precipitated Yttria Stabilized Zirconia (YSZ) to Achieve Translucent Properties," (ONR Report #7), University of Illinois at Urbana-Champaign, Department of Ceramic Engineering, Urbana, IL (November 1982).
4. R. C. Buchanan and D. M. Wilson, "Role of Al_2O_3 in Sintering of Submicron Yttria Stabilized ZrO_2 Powders," (ONR Report #8), University of Illinois, Department of Ceramic Engineering, Urbana, IL (December 1983).
5. R. C. Buchanan and D. M. Wilson, "Densification of Submicron YSZ Powders with Alumina and Borate Additives," (ONR Report #9), University of Illinois, Department of Ceramic Engineering, Urbana, IL (December 1984).
6. R. C. Buchanan and J. Boy, "Effect of Powder Characteristics on Microstructure and Properties in Alkoxide Prepared PZT Ceramics," (ONR Report #10), University of Illinois, Department of Ceramic Engineering, Urbana, IL

Thesis

1. G. Wolter, "Properties of Hot-Pressed ZrV_2O_7 ," M.S. Thesis, University of Illinois, Department of Ceramic Engineering, Urbana, IL, 1981.
2. H. D. DeFord, "Low Temperature Densification of Zirconium Dioxide with Vanadate Additives," M.S. Thesis, University of Illinois, Department of Ceramic Engineering, Urbana, IL, 1982.
3. J. H. Boy, "Effect of Coprecipitation Parameters on the Powder Characteristics of Lead Zirconate Titanate Prepared for Lead Oxide and Butoxide Precursors," M.S. Thesis, University of Illinois, Department of Ceramic Engineering, Urbana, IL, 1983.
4. R. DiChiara, "Processing and Additive Effects on Densification of Calcia Stabilized Zirconia (YSZ)," M.S. Thesis, University of Illinois, Department of Ceramic Engineering, Urbana, IL, 1983.

5. D. M. Wilson, "Effect of Aluminium and Boron oxides on Densification of Yttria Stabilized Zirconia," M.S. Thesis, University of Illinois, Department of Ceramic Engineering, Urbana, IL, 1984.
6. Alena K. Maurice, "Powder Synthesis, Stoichiometry and Processing Effects on Properties of High Purity Barium Titanate," M.S. Thesis, University of Illinois, Department of Ceramic Engineering, Urbana, IL, 1984.
7. S. G. Pope, "Development of Electron Beam Interactive Ceramic Films by RF Sputtering for Memory Applications," M.S. Thesis, University of Illinois, Department of Ceramic Engineering, Urbana, IL, 1984.

Papers

1. D. E. Wittmer and R. C. Buchanan, "Low Temperature Densification of Lead Zirconate Titanate with Vanadium Pentoxide Additive," J. Am. Ceram. Soc., 64 [8] 485-490 (1981).
2. R. C. Buchanan and S. Pope, "Optical and Electrical Properties of Yttria Stabilized Zirconia (YSZ) Crystals," J. Electrochem. Soc., 130, [4] 962-966 (1982).
3. R. C. Buchanan and J. Boy, "Effect of Coprecipitation Parameters on Powder Characteristics and On Densification of PZT Ceramics," Proc. of U.S. Japan Seminar on Dielectrics and Piezoelectrics, Tokyo, Japan, 1982.
4. A. F. Grandin de l'Eprevier and R. C. Buchanan, "Preparation and Properties of $\text{Ca}_2\text{V}_2\text{O}_7$ Single Crystals," J. Electrochem. Soc., 129 [11] 2562-2565 (1982).
5. A. Sircar and R. C. Buchanan, "Densification of CaO -stabilized ZrO_2 with Borate Additives," J. Am. Ceram., 66 [2] 20-21 (1983).
6. G. Wolter and R. C. Buchanan, "Properties of Hot-Pressed ZrV_2O_7 ," J. Electrochem. Soc., 130 [9] 1905-1910 (1983).
7. R. C. Buchanan, H. D. DeFord, and R. W. Doser, "Effects of Vanadate Phase on Sintering and Properties of Monoclinic ZrO_2 ," Advances in Ceramics, Vol 7, pp. 196-207, in: Additives and Interfaces in Electronic Ceramics, Am. Ceram. Soc., Columbus, OH (1984).
8. R. C. Buchanan and D. M. Wilson, "Role of Al_2O_3 in Sintering of Yttria Stabilized ZrO_2 Powders," Adv. in Ceramics, Vol. 12, pp. 431-440 [MgO/ Al_2O_3 Defect Sintering], Am. Ceram. Society, Columbus, OH (1984).
9. R. C. Buchanan and D. M. Wilson, "Densification of Submicron YSZ Powders with Alumina and Borate Additives," J. Am. Ceram. Soc., 1984 (submitted).
10. R. C. Buchanan and J. Boy, "Effect of Powder Characteristics on Microstructure and Properties in Alkoxide Prepared PZT Ceramics," J. Electrochem. Soc. (1984) (submitted).

Technical Presentations Made (1984)

1. Argonne National Laboratory—"Processing of Submicron Zirconia Powders to Achieve Translucent Properties," 2 h Seminar, (Jan. 1984).
2. Materials Research Conference, "Chemical Synthesis Methods for BaTiO_3 and ZrV_2O_7 and Effects on Microstructure and Properties," (Better Ceramics through Chemistry), Albuquerque, N.M. (Feb. 1984). (Poster Presentation).
3. Ferro Corporation, Cleveland, OH, "Review of Chemical Preparation Methods and Processing Parameters for BaTiO_3 Powders," Technical Seminar (Feb, 1984).
4. NICE SHORT COURSE, Lecture Presentation on "Synthesis Parameters and Sintering of Ferroelectric Ceramics," (Pittsburgh, PA, April, 1984).
5. American Ceramic Society (Annual Meetings, Pittsburgh, PA, May, 1984). Three technical papers presented: 1) Sol Gel Processing of Thin Dielectric Films from Colloid Precursors; 2) Effect of Al_2O_3 on Strength of Sintered ZrO_2 ; 3) Processing and Synthesis Effects in High Purity BaTiO_3 .
6. Ohio State University, Columbus, OH (May, 1984). "Microstructure Development and Grain Boundary Effects in BaTiO_3 ," (Technical Seminar).
7. Center for Professional Advancement, (E. Brunswick, N.J.), Course Director for "Ceramic Applications in Electronics," Five (2-h) Lectures: a) Electronic Ceramics/Dielectrics Properties, b) Glasses and Substrates in Electronics, c) Thick Film Hybrid Circuits; d) Magnetic Ceramics (Ferrites), e) Processing of Electronic Ceramics.
8. GTE Sylvania (Exeter, N.H., September, 1984), 2h Technical Seminar on "Ceramic Sensors, Processing and Future Developments."
9. Pennsylvania State University (State College, PA, Oct., 1984), ONR Technical Review Session, "Processing of Ferroelectric and ZrO_2 Ceramics for Optimal Dielectric and Strength Properties."
10. American Ceramic Society (Pacific Coast Joint Meeting, San Francisco, Nov., 1984). "Processing and Additive Effects on Microstructure and Dielectric Properties of High Purity BaTiO_3 ."
11. US-Japan Seminar on Ferroelectric and Piezoelectric Ceramics (Williamsburg, VA, Nov. 1984), Invited Technical Presentation, "Piezoelectronics, Current Practice and Future Prospects," Poster Presentation, "Grain Boundary Effects on Dielectric Properties of BaTiO_3 ."

END

FILMED

2-85

DTIC